Inorg. Chem. **2005**, *44*, 5677–5685

Efficient Red-Emitting Cyclometalated Iridium(III) Complexes Containing Lepidine-Based Ligands

K. R. Justin Thomas,[†] Marappan Velusamy,[†] Jiann T. Lin,*[,†,‡] Chin-Hsiung Chien,[†] Yu-Tai Tao,*[,†] Yuh S. Wen,[†] Ya-Hui Hu,[§] and Pi-Tai Chou[§]

Institute of Chemistry, Academia Sinica, 115 Nankang, Taipei, Taiwan, Department of Chemistry, National Central University, 320 Chungli, Taiwan, and Department of Chemistry, National Taiwan University, Taipei, Taiwan

Received March 15, 2005

Heteroleptic cyclometalated iridium(III) complexes featuring lepidine-based ligands and acetyl acetone auxiliary ligand are synthesized. Multiple lowest energy absorption bands are observed for these complexes indicating substantial mixing of the singlet and triplet levels. All the complexes emit orange or red color in dichloromethane solutions with lifetimes in the range 1.6–3.7 μs. The emission in the complexes probably originates from the ^{3}MLCT state. The complexes are applied as emitting guests in LED devices of the structure ITO/HTL(BPAPF or NPB)/6% Ir in CBP/BCP/Alq_3/LiF/Al. They exhibit excellent device characteristics with an orange to red EL profile.

Introduction

Considerable progress has been made in the design and synthesis of molecular materials suitable for light-emitting diodes that are regarded as potential replacements in future display equipments.[1,2] Organic materials that possess the functions hole and electron transport, appropriate emission characteristics, and amorphous properties are demonstrated to be useful for the fabrication of light-emitting diodes. The excitons formed in a device operation are composed of 25% singlets and 75% triplets.[3] This limits the efficiency of the devices that contain organic materials as emitter to 25%. In view of this, triplet emitters, particularly the cyclometalated iridium(III) complexes, are considered attractive candidates for electroluminescent devices as they enhance the possibility of reaping both singlet and triplet excitons formed during the device operation.[4−8] This might eventually lead to higher efficiencies. Thompson et al. first applied the iridium(III) complexes in LED applications and recorded excellent external efficiencies.[4] The research on iridium(III) complexes with relevance to their application in LED is focused on two themes. First, designing new cyclometalating ligands or auxiliary ligands has received immense attention in a vein to tune the emission color of the resulting complexes. The iridium(III) complexes known to date largely remained as green or yellow emitters, and pure blue- and red-emitting complexes are scarce. Only recently a few red-emitting isoquinoline,[9] pyrazine,[10] or pyrimidine[11] containing iridum-(III) complexes have been reported.[12,13] The second aspect that gained focus these days involves the identification of suitable host materials for iridium(III) complexes. Carba-

* Authors to whom correspondence should be addressed. E-mail: jtlin@chem.sinica.edu.tw (J.T.L.). Fax: 886-2-27831237 (J.T.L.).
† Academia Sinica.
‡ National Central University.
§ National Taiwan University.

(1) Muller, C. D.; Falcou, A.; Reckefuss, N.; Rojahn, M.; Wiederhirn, V.; Rudati, P.; Frohne, H.; Nuyken, O.; Becker, H.; Meerholz, K. *Nature* **2003**, *421*, 829.
(2) Kulkarni, P.; Tonozola, C. J.; Babel, A.; Janekhe, S. A. *Chem. Mater*. **2004**, *16*, 4556.
(3) Baldo, M. A.; O'Brien, D. F.; Thompson, M. E.; Forrest, S. R. *Phys. Rev. B* **1999**, *60*, 14422.
(4) (a) Adachi, C.; Baldo, M. A.; Thompson, M. E.; Forrest, S. R. *J. Appl. Phys*. **2001**, *90*, 5048. (b) Lamansky, S.; Djurovich, P.; Murphy, D.; Abdel-Razzaq, F.; Lee, H. E.; Adachi, C.; Burrows, P. E.; Forrest, S. R.; Thompson, M. E. *J. Am. Chem. Soc*. **2001**, *123*, 4304.
(5) Huang, W. S.; Lin, J. T.; Chien, C. H.; Tao, Y.-T.; Sun, S. S.; Wen, Y. S. *Chem. Mater*. **2004**, *16*, 2480.
(6) (a) Yang, C. H.; Fang, K. H.; Chen C. H.; Sun, I. W. *Chem. Commun*. **2004**, 2232. (b) Coppo, P.; Plummer, E. A.; De Cola, L. *Chem. Commun*. **2004**, 1774.
(7) Nazeeruddin, M. K.; Humphry-Baker, R.; Berner, D.; Rivier, S.; Zuppiroli, L.; Gratzel, M. *J. Am. Chem. Soc*. **2003**, *125*, 8790.
(8) Slinker, J. D.; Gorodetsky, A. A.; Lowry, M. S.; Wang, J. J.; Parker, S.; Rohl, R.; Bernhard, S.; Malliaras, G. G. *J. Am. Chem. Soc*. **2004**, *126*, 2763.
(9) (a) Jiang, C. Y.; Yang, W.; Peng, J. B.; Xiao, S.; Cao, Y. *Adv. Mater*. **2004**, *16*, 537. (b) Yang, C. H.; Tai, C. C.; Sun, I. W. *J. Mater. Chem*. **2004**, *14*, 947.
(10) Duan, J. P.; Sun, P. P.; Cheng, C. H. *Adv. Mater*. **2003**, *15*, 224.
(11) Niu, Y. H.; Chen, B. Q.; Liu, S.; Yip, H.; Bardecker, J.; Jen, A. K. Y.; Kavitha, J.; Chi, Y.; Shu, C. F.; Tseng, Y. H.; Chien, C. H. *Appl. Phys. Lett*. **2004**, *85*, 1619.

10.1021/ic050385s CCC: $30.25
Published on Web 07/06/2005

zole[14] and triazine[15] based amorphous materials have been suggested to possess suitable triplet energies to serve as hosts for these potential triplet emitters. A biphenyl-bridged dicarbazole, 4,4′-*N*,*N*′′-dicarbazolebiphenyl (CBP), is widely used as a host of the fabrication of iridium complex based electroluminescent devices. Besides the usage in LEDs, the cyclometalated iridium(III) complexes have attracted great interest in recent years owing to their use as biological labeling reagents,[16] oxygen sensors,[17] and intermediates in catalytic C−H activation reactions.[18]

In this paper, we adventure on the first theme and report a series of lepidine-based iridium(III) complexes that emit either orange or red color both in steady-state emission and electroluminescence. Though isoquinoline-based iridium(III) complexes have been reported recently,[9] a systematic study of the cyclometalated iridium(III) complexes derived from the quinoline motif is missing.[19] In this paper we develop a new clean and facile synthetic protocol for the synthesis of a series of lepidine-based ligands using the Suzuki protocol. We attach a variety of aromatic segments on the lepidine nucleus to arrive at a series of ligands. The complexes prepared using these ligands are strongly emissive at room temperature. We also have undertaken crystal structure analysis for three complexes, and a comparative evaluation of the bonding parameters is also attempted. Finally, the usefulness of these complexes as triplet emitters in electroluminescent devices was examined by applying them as guests in CBP hosts in two different multilayered device architectures. All the devices led to bright orange or red color emission.

Experimental Section

General Information. All reactions and manipulations were carried out under N_2 with the use of standard inert atmosphere and Schlenk techniques. Solvents were dried by standard procedures. All column chromatography was performed under N_2 with the use of silica gel (230−400 mesh, Macherey-Nagel GmbH & Co.) as the stationary phase in a column of 30 cm long and 2.0 cm diameter. The ^{1}H NMR spectra were measured by using Bruker AC300 or AMX400 spectrometer. Mass spectra were recorded on a JMS-700 double focusing mass spectrometer (JEOL, Tokyo, Japan). Elemental analyses were performed on a Perkin-Elmer 2400 CHN analyzer. Cyclic voltammetry experiments were performed with a BAS-100 electrochemical analyzer. All measurements were carried out at room temperature with a conventional three-electrode configuration consisting of a glassy carbon working electrode, a platinum wire auxiliary electrode, and a nonaqueous $Ag/AgNO_3$ reference electrode. The $E_{1/2}$ values were determined as $1/2(E_p^a + E_p^c)$, where E_p^a and E_p^c are the anodic and cathodic peak potentials, respectively. The potentials are quoted against the ferrocene internal standard. The solvent in all experiments was dichloromethane, and the supporting electrolyte was 0.1 M tetrabutylammonium hexafluorophosphate. Electronic absorption spectra were obtained on a Perkin-Elmer Lambda 900 UV−vis−NIR spectrophotometer for dichloromethane solutions. Emission spectra were recorded in deoxygenated toluene solution at 298 K with an Jobin Yvon SPEX Fluorolog-3 spectrofluorometer. The emission spectra were collected on samples with o.d. < 0.1 at the excitation wavelength. The spectra were corrected for instrumental response. UV−visible spectra were checked before and after irradiation to monitor possible sample degradation. Emission maxima were reproducible to within 2 nm. Luminescence quantum yields (Φ_{em}) were calculated using Coumarin 1 as primary standard ($\Phi_{em} = 0.99$ in ethyl acetate) and Ir(ppy)$_3$ ($\Phi_{em} = 0.40$ in toluene) as secondary reference.[20] Luminescence quantum yields were taken as the average of three separate determinations and were reproducible to within 10%. The lifetime was measured with the laser photolysis technique in which the third harmonic of an Nd:YAG laser (8 ns, Continuum Surlite II) was used as the excitation source, coupled with a fast response photomultiplier (Hamamatsu model R5509-72) operated at −80 °C. Typically an average of 512 shots were acquired for each measurement.

Preparation of the Ligands. The ligands were prepared by essentially following the same procedure so an illustrative example is provided below for BuL.

2-(4-*tert*-Butylphenyl)-4-methylquinoline (BuL). A mixture of 2-chlorolepidine (1.78 g, 10 mmol), 4-*tert*-butylphenylboronic acid (2.67 g, 15 mmol), $Pd(PPh_3)_4$ (1.16 g, 1 mmol, 10 mol %), anhydrous sodium carbonate (1.59 g, 15 mmol), tetrahydrofuran (20 mL), toluene (20 mL), and water (5 mL) was heated under nitrogen atmosphere at 80 °C for 24 h. At the end of the time, the reaction mixture was diluted with an additional 20 mL of water and the organic layer separated was collected. It was dried to leave a colorless liquid, adsorbed on silica gel, and purified by column chromatography using hexane/dichloromethane mixture (1:1). A colorless liquid solidified on standing. Yield: 2.48 g (90%). ^{1}H NMR (δ, $CDCl_3$): 1.39 (s, 9 H), 2.73 (s, 3 H), 7.49−7.57 (m, 3 H), 7.67−7.73 (m, 2 H), 7.97 (d, $J = 7.8$ Hz, 1 H), 8.07−8.10 (m, 2 H), 8.18 (d, $J = 8.2$ Hz, 1 H). HRMS: calcd for $C_{20}H_{22}N$ (M + H), 276.1752; found, 276.1753.

2-(4-(Trifluoromethyl)phenyl)-4-methylquinoline (CF_3L). A colorless liquid solidified on standing. Yield: 82%. ^{1}H NMR (δ, $CDCl_3$): 2.74 (s, 3 H), 7.53−7.57 (m, 1 H), 7.67−7.75 (m, 4 H), 7.97 (d, $J = 8.2$ Hz, 1 H), 8.17 (d, $J = 8.2$ Hz, 1 H), 8.24 (d, $J =$

(12) For homoleptic red-emitting iridium complexes, see: Tsuboyama, A.; Iwawaki, H.; Furugori, M.; Mukaide, T.; Kamatani, J.; Igawa, S.; Moriyama, T.; Miura, S.; Takiguchi, T.; Okada, S.; Hoshino, M.; Ueno, K. *J. Am. Chem. Soc.* **2003**, *125*, 12971.

(13) For red-emitting iridium complexes grafted on polymers, see: (a) Sandee, A. J.; Williams, C. K.; Evans, N. R.; Davies, J. E.; Boothby, C. E.; Kohler, A.; Friend, R. H.; Holmes, A. B. *J. Am. Chem. Soc.* **2004**, *126*, 7041. (b) Chen, X. W.; Liao, J. L.; Liang, Y. M.; Ahmed, M. O.; Tseng, H. E.; Chen, S. A. *J. Am. Chem. Soc.* **2003**, *125*, 636.

(14) (a) van Dijken, A.; Bastiaansen, J. J. A. M.; Kiggen, N. M. M.; Langeveld, B. M. W.; Rothe, C.; Monkman, A.; Bach, I.; Stossel, P.; Brunner, K. *J. Am. Chem. Soc.* **2004**, *126*, 7718. (b) Brunner, K.; van Dijken, A.; Borner, H.; Bastiaansen, J. J. A. M.; Kiggen, N. M. M.; Langeveld, B. M. W. *J. Am. Chem. Soc.* **2004**, *126*, 6035.

(15) Inomata, H.; Goushi, K.; Masuko, T.; Konno, T.; Imai, T.; Sasabe, H.; Brown, J. J.; Adachi, C. *Chem. Mater.* **2004**, *16*, 1285.

(16) (a) Lo, K. K. W.; Chan, J. S. W.; Lui, L. H.; Chung, C. K. *Organometallics* **2004**, *23*, 3108. (b) Lo, K. K. W.; Chung, C. K.; Lee, T. K. M.; Lui, L. H.; Tsang, K. H. K.; Zhu, N. Y. *Inorg. Chem.* **2003**, *42*, 6886.

(17) (a) DeRosa, M. C.; Hodgson, D. J.; Enright, G. D.; Dawson, B.; Evans, C. E. B.; Crutchley, R. J. *J. Am. Chem. Soc.* **2004**, *126*, 7619. (b) DeRosa, M. C.; Mosher, P. J.; Yap, G. P. A.; Focsaneanu, K. S.; Crutchley, R. J.; Evans, C. E. B. *Inorg. Chem.* **2003**, *42*, 4864. (c) Gao, R. M.; Ho, D. G.; Hernandez, B.; Selke, M.; Murphy, D.; Djurovich, P. I.; Thompson, M. E. *J. Am. Chem. Soc.* **2002**, *124*, 14828.

(18) (a) Oxgaard, J.; Muller, R. P.; Goddard, W. A.; Periana, R. A. *J. Am. Chem. Soc.* **2004**, *126*, 352. (b) Periana, R. A.; Liu, X. Y.; Bhalla, G. C. *Chem. Commun.* **2002**, 3000.

(19) While the manuscript was under preparation, a paper describing the iridium complexes of 4-phenylquinoline-based ligands has been appeared. See: Wu, F.-I.; Su, H.-J.; Shu, S.-F.; Luo, L.; Diau, W.-G.; Cheng, C.-H.; Duan, J.-P.; Lee, G.-H. *J. Mater. Chem.* **2005**, *15*, 1035.

(20) Tsuboyama, A.; Iwawaki, H.; Furugori, M.; Mukaide, T.; Kamatani, J.; Iawa, S.; Moriyama, T.; Miura, S.; Takiguchi, T.; Okada, S.; Hoshino, M.; Ueno, K. *J. Am. Chem. Soc.* **2003**, *125*, 12971.

7.7 Hz, 2 H). HRMS: calcd for $C_{17}H_{13}NF_3$ (M + H): 288.1000; found, 288.0992.

***N,N*-Dimethyl-4-(4-methylquinolin-2-yl)benzenamine (NMe_2L).** A pale yellow solid formed. Yield: 64%. ^{1}H NMR (δ, $CDCl_3$): 2.72 (s, 3 H), 3.03 (s, 6 H), 6.80−6.84 (m, 2 H), 7.42−7.48 (m, 1 H), 7.63−7.68 (m, 2 H), 7.93 (d, J = 7.8 Hz, 1 H), 8.07−8.13 (m, 3 H). HRMS: calcd for $C_{18}H_{19}N_2$ (M + H), 263.1548; found, 263.1547.

***N*-(4-(4-Methylquinolin-2-yl)phenyl)-*N*-phenylbenzenamine (NPh_2L).** A pale yellow solid formed. Yield: 79%. ^{1}H NMR (δ, $CDCl_3$): 2.74 (s, 3 H), 7.06 (t, J = 7.3 Hz, 2 H), 7.15−7.21 (m, 6 H), 7.26−7.31 (m, 4 H), 7.48−7.53 (m, 1 H), 7.66−7.72 (m, 2 H), 7.97 (d, J = 8.2 Hz, 1 H), 8.00−8.04 (m, 2 H), 8.15 (d, J = 8.2 Hz, 1 H). HRMS: calcd for $C_{28}H_{23}N_2$ (M + H), 387.1861; found, 387.1855.

4-Methyl-2-(naphthalen-1-yl)quinoline (NapL). Yield: 76%. A colorless solid formed. ^{1}H NMR (δ, $CDCl_3$): 2.78 (s, 3 H), 7.42−7.53 (m, 2 H), 7.55−7.63 (m, 3 H), 7.68−7.78 (m, 2H), 7.90−7.94 (m, 2 H), 8.05−8.12 (m, 2 H), 8.24 (d, J = 8.2 Hz, 1 H). HRMS: calcd for $C_{20}H_{16}N$ (M + H), 270.1283; found, 270.1278.

4-Methyl-2-(phenanthren-10-yl)quinoline (PhenL). A colorless solid formed. Yield: 71%. ^{1}H NMR (δ, $CDCl_3$): 2.80 (s, 3 H), 7.52−7.71 (m, 6 H), 7.75−7.80 (m, 1 H), 7.93−7.96 (m, 2 H), 8.07−8.11 (m, 2 H), 8.26 (d, J = 8.2 Hz, 1 H), 8.73 (d, J = 8.2 Hz, 1 H), 8.78 (d, J = 8.2 Hz, 1 H). HRMS: calcd for $C_{24}H_{18}N$ (M + H), 320.1439; found, 320.1439.

Preparation of the Complexes (1−6). All the cyclometalated iridium(III) complexes were prepared by essentially following the same procedure so an illustrative example is provided below for **1**.

Ir(BuL)$_2$(acac) (1). A mixture of 2-(4-*tert*-butylphenyl)-4-methylquinoline (BuL) (0.826 g, 3 mmol), anhydrous $IrCl_3$ (299 mg, 1 mmol), 2-methoxyethanol (6 mL), and distilled water (3 mL) was heated at reflux for 12 h. After cooling, the brown precipitate formed was filtered out and washed thoroughly with methanol (50 mL), diethyl ether (50 mL), and hexane (20 mL). The dried chloro-bridged dimer was suspended in 2-methoxyethanol (10 mL) and treated with acetyl acetone (200 mg, 2 mmol) and anhydrous Na_2CO_3 (315 mg, 3 mmol). The reaction mixture was stirred at 80 °C for 8 h. The insoluble products were filtered out, washed with water (10 mL), methanol (10 mL), and diethyl ether (20 mL), and dried. They were dissolved again in dichloromethane (20 mL) and adsorbed on silica gel and rapidly purified by column chromatography using hexane/dichloromethane mixture (3:2). The red solid obtained was recrystallized from a dichloromethane/hexane mixture. Red needles formed. Yield: 685 mg (82%). ^{1}H NMR (δ, $CDCl_3$): 0.86 (s, 18 H), 1.50 (s, 6 H), 2.90 (s, 6 H), 4.64 (s, 1 H), 6.49 (s, 2 H), 6.91 (d, J = 7.3 Hz, 2 H), 7.32−7.37 (m, 2 H), 7.41−7.45 (m, 2 H), 6.71 (d, J = 8.2 Hz, 2 H), 7.85 (s, 2 H), 7.90 (d, J = 8.2 Hz, 2 H), 8.47 (d, J = 8.7 Hz, 2 H). FAB MS: m/z 840.1 (M^+). Anal. Calcd for $C_{45}H_{47}IrN_2O_2$: C, 64.34; H, 5.64; N, 3.33. Found: C, 64.35; H, 5.58; N, 3.15.

Ir(CF_3L)$_2$(acac) (2). A red microcrystalline solid formed. Yield: 77%. ^{1}H NMR (δ, $CDCl_3$): 1.46 (s, 6 H), 2.95 (s, 6 H), 4.59 (s, 1 H), 6.69 (s, 2 H), 7.17 (d, J = 8.8 Hz, 2 H), 7.48−7.54 (m, 4 H), 7.87 (d, J = 8.2 Hz, 2 H), 7.94−7.97 (m, 4 H), 8.35 (d, J = 8.7 Hz, 2 H). FAB MS: m/z 863.9 (M^+). Anal. Calcd for $C_{39}H_{29}F_6IrN_2O_2$: C, 54.22; H, 3.38; N, 3.24. Found: C, 54.19; H, 3.12; N, 3.0.

Ir(NMe_2L)$_2$(acac) (3). Red crystals formed. Yield: 56%. ^{1}H NMR (δ, $CDCl_3$): 1.47 (s, 6 H), 2.49 (s, 12 H), 2.82 (s, 6 H), 4.68 (s, 1 H), 5.83 (s, 2 H), 6.31 (d, J = 7.5 Hz, 2 H), 7.31−7.38 (m, 4 H), 7.59 (d, J = 8.2 Hz, 2 H), 7.68 (s, 2 H), 7.80−7.83 (m, 2 H), 8.52−8.55 (m, 2 H). FAB MS: m/z 814.1 (M^+). Anal. Calcd for $C_{41}H_{41}IrN_4O_2$: C, 60.50; H, 5.08; N, 6.88. Found: C, 59.75; H, 4.82; N, 6.69.

Ir(NPh_2L)$_2$(acac) (4). A red solid formed. Yield: 65%. ^{1}H NMR (δ, $CDCl_3$): 1.51 (s, 6 H), 2.74 (s, 6 H), 4.65 (s, 1 H), 6.11 (s, 2 H), 6.51 (d, J = 7.5 Hz, 2 H), 6.76−6.87 (m, 20 H), 7.43−7.56 (m, 8 H), 7.80 (d, J = 8.2 Hz, 2 H), 8.43 (d, J = 8.2 Hz, 2 H). FAB MS: m/z 1062.0 (M^+). Anal. Calcd for $C_{61}H_{49}IrN_4O_2$: C, 68.97; H, 4.65; N, 5.27. Found: C, 69.07; H, 4.47; N, 5.09.

Ir(NapL)$_2$(acac) (5). Dark brown crystals formed. Yield: 88%. ^{1}H NMR (δ, $CDCl_3$): 1.43 (s, 6 H), 2.94 (s, 6 H), 4.54 (s, 1 H), 6.73 (d, J = 8.2 Hz, 2 H), 6.96 (d, J = 8.4 Hz, 2 H), 7.25−7.37 (m, 4 H), 7.44−7.53 (m, 4 H), 7.64 (d, J = 8.2 Hz, 2 H), 7.94 (dd, J = 8.2, 1.2 Hz, 2 H), 8.30 (d, J = 8.2 Hz, 2 H), 8.52 (s, 2 H), 8.69 (d, J = 8.7 Hz, 2 H). FAB MS: m/z 828.0 (M^+). Anal. Calcd for $C_{45}H_{35}IrN_2O_2$: C, 65.28; H, 4.26; N, 3.38. Found: 65.09; H, 4.11; N, 3.18.

Ir(PhenL)$_2$(acac) (6). A dark brown powder formed. Yield: 84%. ^{1}H NMR (δ, $CDCl_3$): 1.51 (s, 6 H), 2.81 (s, 6 H), 4.60 (s, 1 H), 6.29−6.31 (m, 4 H), 6.81−6.87 (m, 2 H), 7.00−7.06 (m, 2 H), 7.12 (t, J = 7.9 Hz, 2 H), 7.33 (d, J = 8.2 Hz, 2 H), 7.56(t, J = 7.5 Hz, 2 H), 7.68−7.76 (m, 4 H), 8.29 (d, J = 8.2 Hz, 2 H), 8.62−8.66 (m, 4 H), 8.87 (d, J = 8.2 Hz, 2 H). FAB MS: m/z 928.0 (M^+). Anal. Calcd for $C_{53}H_{39}IrN_2O_2$: C, 68.59; H, 4.24; N, 3.02. Found: C, 68.51; H, 3.97, N, 2.92.

Structural Determination of Ir(CF_3L)$_2$(acac) (2), Ir(NMe_2L)$_2$-(acac) (3), and (NapL)$_2$Ir(acac) (5). Crystals of **2** (red plate, dimensions 0.32 × 0.22 × 0.16 mm), **3**, (red plate, dimensions 0.36 × 0.20 × 0.18 mm), and **5** (dark red prism, dimensions 0.22 × 0.18 × 0.16 mm) were grown from a dichloromethane solution layered with hexane at room temperature. Relevant crystal data are summarized in Tables S1, S4, and S7 (Supporting Information). The space groups triclinic $P\bar{1}$ (for **2**) and monoclinic $P2_1/n$ (for **3** and **5**) were determined from systematic absence of specific reflections; successful refinement of the structure confirmed the space group assignment. Direct methods were used to locate the Ir atom, whereas subsequent cycles of least-squares refinements and difference Fourier maps were used to locate the remaining non-hydrogen atoms. Hydrogen atoms were placed at calculated positions. Fluorine positions in one of the CF_3 groups in compound **2** were found to be disordered and modeled with fractional occupancies. All calculations were performed using the SHELX software package.

LEDs Fabrication and Measurements. Compound BCP (2.9-dimethyl-4,7-diphenyl-1,10-phenanthroline) was purchased from Aldrich and used as received. Compounds Alq_3 (tris(8-hydroxyquinolinato)aluminum),[21] NPB (4,4′-bis{*N*-(1-naphthyl-*N*-phenylamino)biphenyl}),[22] CBP (4,4′-*N*,*N*′-dicarbazolebiphenyl),[22] and BPAPF (9,9-bis{4-[bis(*p*-biphenyl)aminophenyl]}fluorene)[23] were synthesized according to literature procedures and were sublimed twice prior to use. Prepatterned ITO substrates with an effective individual device area of 3.14 mm^2 were cleaned as described in a previous report.[24] A 40-nm-thick film of BPAPF or NPB was deposited first as the hole transport layer (HTL). The light-emitting layer (30 nm) was then deposited by coevaporating a CBP host and a phosphorescent dopant (∼6% dopant concentration), with both deposition rates being controlled with two independent quartz crystal oscillators. A 10-nm-thick BCP as a hole and exciton

(21) Chen, C. H.; Shi, J. *Coord. Chem. Rev.* **1998**, *171*, 161.
(22) Koene, B. E.; Loy, D. E.; Thompson, M. E. *Chem. Mater.* **1998**, *10*, 2235.
(23) Ko, C.-W.; Tao, Y.-T. *Synth. Met.* **2002**, *126*, 37.
(24) Balasubramaniam, E.; Tao, Y. T.; Danel, A.; Tomasik, P. *Chem. Mater.* **2000**, *12*, 2788.

Scheme 1. Synthesis of the Complexes

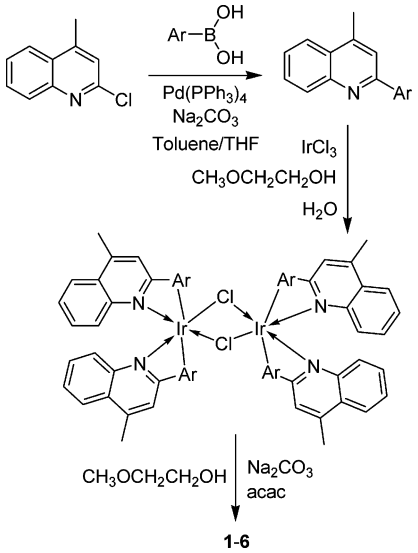

blocking layer (HBL) and 30-nm-thick Alq_3 as an electron transport layer were then deposited sequentially. Finally, a thin layer of LiF (5 Å) followed by aluminum (500 Å) was deposited as the cathode, which was capped with 1000 Å of silver. *I*−*V* curves were measured on a Keithley 2400 Source meter in ambient environment. Light intensity was measured with a Newport 1835 optical meter.

Results and Discussion

Synthesis of the Ligands and the Complexes. The Suzuki coupling reactions between commercially available 2-chlorolepidine and the corresponding aryl boronic acids afforded the ligands required for this study (Scheme 1). C−C-coupling reactions involving Suzuki protocol had not been realized earlier for 2-chlorolepidine. However, Negishi coupling reactions were successfully demonstrated recently on 2-chlorolepidine to arrive at bipyridine-like chelating ligands.[25] Facile reactivity of chlorolepidine is similar to that observed for chloropyridine in analogous reactions.[26] Complexes depicted in Figure 1 were obtained in moderate to good yields from the above ligands by a conventional two-step sequence (Scheme 1). In the first step a chloro-bridged dimer was formed by the reaction of the ligand with $IrCl_3$. This dimer was cleaved by treatment with acetylacetone in the presence of Na_2CO_3 to produce the monomeric heteroleptic complexes. The complexes were characterized by NMR and mass spectra, by elemental analyses, and in the case of **2**, **3**, and **5** by single-crystal X-ray diffraction. In the complexes, the acetylacetonate *CH* protons appear in the region 4.54−4.68 ppm as a sharp singlet. For the complexes possessing arylpyridine cyclometalating ligands this signal is reported to appear at >5.1 ppm.[4b] In the complex $Ir(PQ)_2(acac)$ [where PQ = 2-phenylquinoline], the signal attributable to the acetylacetonate *CH* proton is located at 4.7 ppm.[4b] All these facts clearly point that in quinoline-based cyclometalating iridium complexes the acetylacetonate *CH* protons are more shielded due to the larger electron density on Ir center. This obviously is the result of weaker ligand field strength of

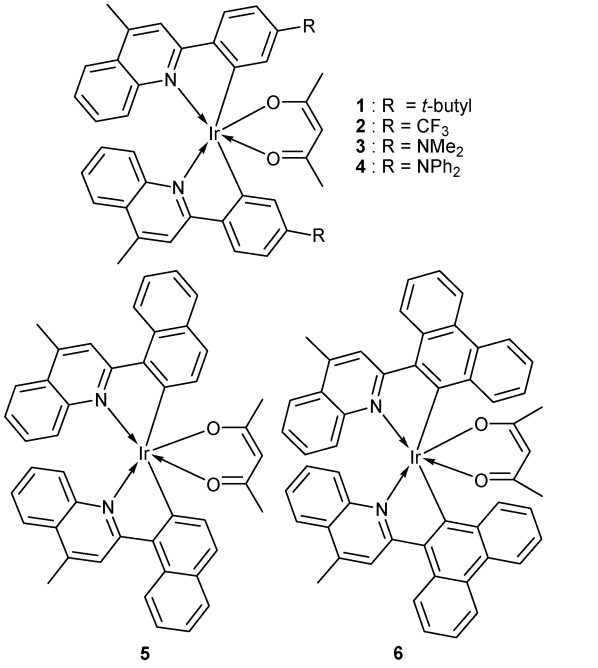

Figure 1. Structure of the complexes.

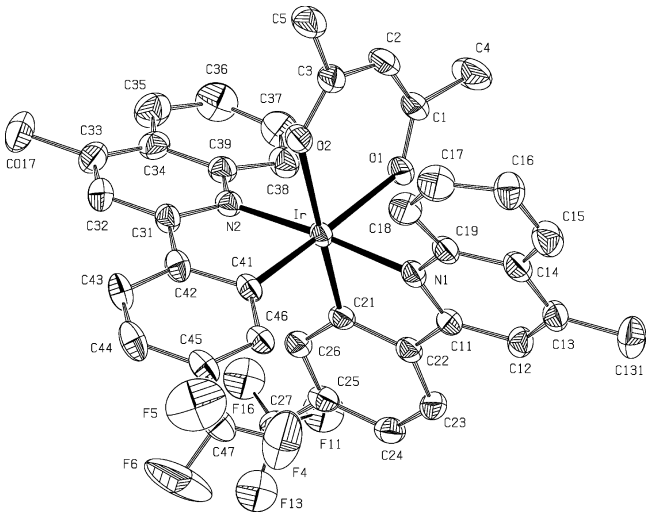

Figure 2. ORTEP diagram of the complex $Ir(CF_3L)_2(acac)$ (**2**).

quinoline that inhibits effective back-donation. It is interesting to note here that the closely analogous isoquinoline systems led to low field signals ca. 5.2 ppm.[9b] The above-mentioned shielding effect is also manifested on the chemical shift of the acetylacetonate CH_3 protons. In arylpridine complexes they are observed above 1.6 ppm, while in the present complexes they resonate between 1.43 and 1.51 ppm.

Crystal Structures of the Complexes $Ir(CF_3L)_2(acac)$ (2), $Ir(NMe_2L)_2(acac)$ (3), and $Ir(NapL)_2(acac)$ (5). ORTEP plot of the compounds **2**, **3**, and **5** are displayed in Figures 2−4, respectively, and the coordination geometrical parameters are listed in Table 1. In general, the iridium(III) center adopts a distorted octahedral geometry with the cis-O,O, cis-C,C, and trans-N,N chelate disposition, and the angles of the trans ligands at the metal center range between 173.1(3) and 177.6(2) Å. Incidentally, the limiting trans angles (N−Ir−N and C−Ir−O) were observed for the naphthyl-substituted complex, **5**. The shortest coordination distances

(25) Fang, Y. Q.; Hanan, G. S. *Synlett* **2003**, 852.
(26) Tagata, T.; Nishida, M. *J. Org. Chem.* **2003**, *68*, 9412.

Table 1. Coordination Bonding Parameters (Å, deg) Observed in Complexes **2**, **3**, and **5**

compd	Ir−C	Ir−N	Ir−O	C−Ir−C	N−Ir−N	O−Ir−O	C−Ir−O	N−Ir−O	C−Ir−N
$Ir(CF_3L)_2(acac)$ (**2**)	1.975(12)	2.082(11)	2.161(8)	93.6(5)	175.5(3)	86.6(4)	90.8(4)	101.8(4)	95.7(5)
	1.976(12)	2.054(11)	2.177(9)				89.1(4)	101.1(4)	97.9(5)
							175.0(3)	80.4(4)	80.9(5)
							176.6(4)	82.6(4)	80.0(5)
$Ir(NMe_2L)_2(acac)$ (**3**)	1.965(5)	2.068(5)	2.170(4)	94.0(2)	176.35(19)	85.91(15)	174.4(2)	99.89(18)	81.0(2)
	1.982(6)	2.077(5)	2.171(4)				91.3(2)	82.93(17)	98.0(2)
							176.77(19)	101.74(18)	96.5(2)
							88.8(2)	80.85(18)	79.6(2)
$Ir(NapL)_2(acac)$ (**5**)	1.982(8)	2.049(7)	2.145(6)	95.1(3)	177.6(2)	85.6(2)	177.2(3)	100.2(2)	80.0(3)
	1.989(8)	2.061(6)	2.155(5)				87.7(3)	81.9(2)	98.2(3)
							173.1(3)	100.4(2)	99.0(3)
							91.6(3)	80.8(2)	79.7(3)

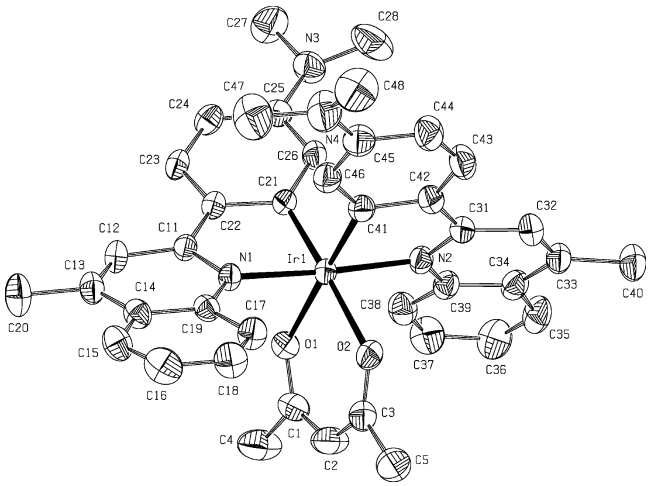

Figure 3. ORTEP diagram of the complex $Ir(NMe_2L)_2(acac)$ (**3**).

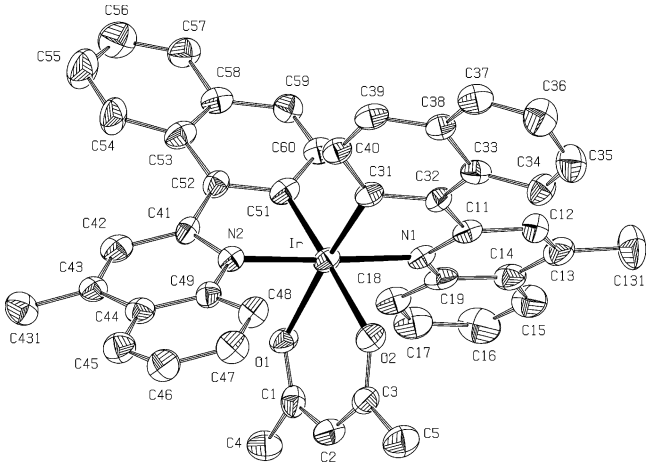

Figure 4. ORTEP plot of the complex $Ir(NapL)_2(acac)$ (**5**).

are associated with the Ir−C bonds with the longest being Ir−O bonds. The average Ir−O bond length observed in the complexes [2.163(6) Å] is considerably longer than the mean Ir−O value of 2.088 Å reported in the Cambridge Crystallographic Database and reflects the pronounced trans influence of the aromatic rings. Among the complexes, naphthyl derivative (**5**) possesses the relatively shorter Ir−O distances [2.150(6) vs 2.170(6) Å] indicative of comparatively weaker *transophobic* behavior.[27] In the three complexes, the C−Ir−C and N−Ir−N bond angles assume the order **2** < **3** < **5**, while the O−Ir−O angles decreases from **2** to **5**. Two sets of N−Ir−O, C−Ir−O, and C−Ir−N angles were observed in the complexes. The larger N−Ir−O and C−Ir−O angles shrink slightly on moving from **2** to **5**, and the reverse is true for the larger C−Ir−N angles. The smaller angles associated with these bonds do not show a significant trend.

A comparison of the structural parameters observed for these complexes with the previously known related complexes is noteworthy. The selected bond lengths and angles for a few recently reported cyclometalated iridium(III) acetylacetonate complexes are listed in Table 2. On inspection of the bonding parameters a few points emerge: (i) Among the complexes, **2** and **3** possess the shorter Ir−C bonds. This indicates a stronger σ-donation from these substituted phenyl ligands. (ii) Similarly the complexes **2** and **3** show relatively longer Ir−N and Ir−O bonds. Weaker Ir−O bonds result from the trans influence exerted by the aryl ligands, while the elongated Ir−N bonds may suggest weaker basicity of quinoline when compared to pyridine. Comparatively longer Ir−N bonds are also observed for the complexes $Ir(btpy\text{-}Br)_2(acac)$[13a] and $Ir(CF_3\text{-}pbtz)_2(acac)$[29] probably due to the same reason. (iii) The complexes **2**, **3**, and **5** exhibit narrower bite angles (86° vs 88−90°) for the acetylacetone chelate. This may be attributed to the steric effect of the bulkier quinoline motif which forces the acetylacetone to confine to the smaller space. This is also supported by the distinctively distorted N−Ir−O angles observed for the above three complexes.

Photophysical Properties. Absorption spectra of the complexes and the ligands were measured in dichloromethane solutions at 298 K. Figure 5 show a comparison of absorption spectra of complexes **1**, **4**, and **6**, and the pertinent data are gathered in Table 3. Except the NMe_2 (NMe_2L) and NPh_2 (NPh_2L) substituted ligands, all the ligands display absorption spectra in the range 250−350 nm (see Figure S2 in the Supporting Information). The ligands NMe_2L and NPh_2L display red-shifted absorption profiles peaking at ca. 375 nm. On the contrary, the absorption spectra of the complexes are dominated by multiple bands originating from ligand-centered $\pi-\pi^*$ transitions and MLCT transitions (Table 3). The bands that appear above 400 nm are believed to be arising from charge-transfer transitions. The observed

(27) Vicente, J.; Arcas, A.; Bautista, D.; de Arellano, M. C. R. *J. Organomet. Chem*. **2002**, *663*, 164.

(28) Lamansky, S.; Djurovich, P.; Murphy, D.; Abdel-Razzaq, F.; Kwong, R.; Tsyba, I.; Bortz, M.; Mmui, B.; Bau, R.; Thompson, M. E. *Inorg. Chem*. **2001**, *40*, 1704.

(29) Laskar, I. R.; Chen. T. M. *Chem. Mater*. **2004**, *16*, 111.

Table 2. Comparison of Average Bond Lengths (Å) and Angles (deg) in Iridium(III) Acetylacetonate Complexes

complex	Ir−C	Ir−N	Ir−O	C−Ir−C	N−Ir−N	O−Ir−O	C−Ir−O	N−Ir−O	C−Ir−N
$Ir(CF_3L)_2(acac)$ (**2**)	1.976(12)	2.068(11)	2.169(9)	93.8(4)	175.5(3)	86.6(4)	175.8(4)	101.5(4)	96.8(5)
							90.0(4)	81.5(4)	80.5(5)
$Ir(NMe_2L)_2(acac)$ (**3**)	1.974(6)	2.073(5)	2.171(4)	94.0(2)	176.4(2)	85.9(2)	175.6(2)	100.8(2)	97.3(2)
							90.1(2)	81.9(2)	80.3(2)
$Ir(NapL)_2(acac)$ (**5**)	1.986(8)	2.055(7)	2.150(6)	95.1(3)	177.6(2)	85.6(2)	175.2(3)	100.3(2)	98.6(3)
							89.7(3)	81.4(2)	79.9(3)
$Ir(ppy)_2(acac)$[28]	2.003(9)	2.010(9)	2.146(6)	95.2(5)	176.3(4)	90.0(3)	175.6(3)	94.5(3)	95.8(4)
							87.5(3)	88.1(3)	81.7(4)
$Ir(tpy)_2(acac)$[28]	1.984(6)	2.032(5)	2.149(4)	93.4(2)	176.2(2)	88.2(2)	173.9(2)	94.3(2)	97.2(2)
							89.5(2)	88.3(2)	80.4(2)
$Ir(btpy\text{-}Br)_2(acac)$[13a]	2.01(2)	2.071(17)	2.136(15)	92.1(8)	177.6(7)	89.8(5)	171.3(7)	93.2(6)	101.7(8)
							89.7(7)	87.0(6)	79.7(8)
$Ir(CF_3\text{-}pbtz)_2(acac)$[29]	1.990(5)	2.055(4)	2.136(3)	93.5(2)	174.7(2)	88.9(1)	176.1(2)	96.6(2)	96.2(2)
							88.9(2)	87.1(2)	80.1(2)
$Ir(fbi)_2(acac)$[5]	2.006(4)	2.038(3)	2.145(3)	93.4(2)	172.7(2)	88.0(2)	174.6(1)	95.1(1)	94.8(2)
							89.5(1)	90.2(1)	80.1(1)
$Ir(cbtz)_2(acac)$[17a]	1.986(2)	2.044(1)	2.133(1)	95.92(7)	176.56(5)	87.68(6)	173.91(6)	94.76(6)	101.93(7)
							88.36(7)	82.96(6)	80.25(7)

Table 3. Physical Parameters for the Complexes

complex	λ_{abs}/nm[a]	λ_{em}/nm[a]	τ, μs[a]	Φ_f[b]	E_{ox}/mV[a,c]	HOMO/eV[d]	LUMO/eV[e]	ΔE/eV[e]
1	345, 420, 465, 505, 545	599	1.6	0.17	266 (68)	5.066	2.908	2.158
2	317, 430, 460, 500, 545	591	1.9	0.36	564 (69)	5.364	3.187	2.177
3	345, 398	598	3.7	0.10	128 (72), 403 (86)	4.928	2.789	2.139
4	366, 405, 502 sh	593	2.4	0.16	237 (83), 544 (68)	5.037	2.916	2.121
5	310, 374, 487, 528 sh	634	1.8	0.18	312 (70)	5.112	3.027	2.085
6	310, 377, 508, 535 sh	663	3.3	0.29	198 (85)	4.998	2.930	2.068

[a] Measured in dichloromethane solution. Concentration for UV measurements: $\sim 2.0 \times 10^{-5}$ M. [b] For emission measurements, toluene solutions with o.d. < 0.1 at excitation wavelength (350 nm) were used. Approximately concentration: $10^{-6}-10^{-7}$ M. [c] Scan rate: 100 mV/s. Electrolyte: 0.1 M tetrabutylammonium hexafluorophosphate. Concentration: 2.5×10^{-4} M. The potentials are quoted against the internal ferrocene standard. [d] Deduced form the equation HOMO = 4.8 + E_{ox}. [e] Calculated from the optical edge and the relation ΔE = HOMO − LUMO.

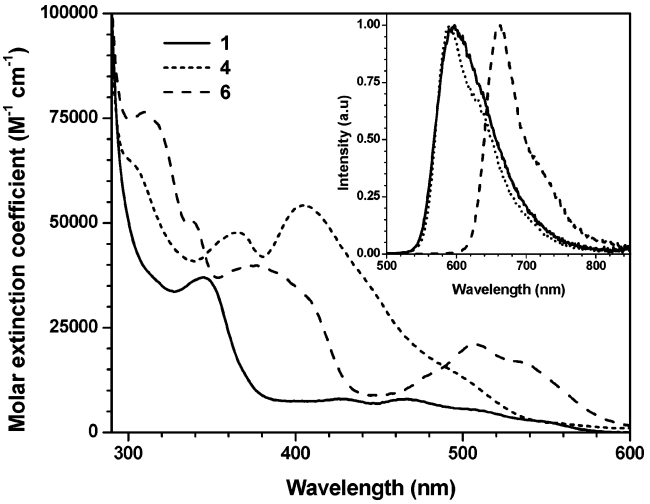

Figure 5. Absorption and emission spectra of the selected complexes, $Ir(BuL)_2(acac)$ (**1**), $Ir(NPh_2L)_2(acac)$ (**4**), and $Ir(PhenL)_2(acac)$ (**6**), recorded in CH_2Cl_2 solutions.

MLCT transitions are weaker, however, clearly resolved for the complexes **1**, **2**, **5**, and **6**. In case of **3** and **4** the red-shifted ligand-based transitions probably overlay the weaker MLCT transitions. For **1** and **2** at least four MLCT transitions are noticed, indicating the presence of multiple close lying MLCT states in these complexes (see for instance Figure 5). For the naphthyl and phenanthrenyl complexes (**5** and **6**) the MLCT transitions appear distinctively above 450 nm with appreciable extinction coefficients (>15 000 M^{-1} cm^{-1}) and suggest substantial mixing of spin forbidden ^{3}MLCT and higher lying ^{1}MLCT transitions by spin−orbit coupling of Ir. In the present complexes, probably the spin−orbit coupling is enhanced by the presence of closely lying $\pi-\pi^*$ and MLCT states and the heavy atom effect.[30] It is interesting to note the changes in the molar extinction coefficient of the low-energy MLCT band that in complex **5** and **6** is two times higher than that of the complex **1** which in turn is 0.5 times higher than that of the CF_3 complex **2**. Electron deficient coligands were found to influence the position and extinction coefficient of the MLCT transitions in cyclometalated iridium(III) complexes. This was identified as a unique pathway for blue-shifting the emission profile.[7] In our complexes, the observed trend in optical density and peak maxima may reflect the trend in the electron-donating capability of the cyclometalating aryl moieties.

All the complexes reported here exhibit moderate to intense phosphorescence at room temperature in degassed toluene solutions with the lifetimes in the range 1.6−3.7 μs. These lifetimes are indicative of strong spin−orbit coupling leading to intersystem crossing from the singlet to the triplet state.[30] Hence, we believe that in these complexes the emission originates from the triplet states. It seems that the cyclometalating aromatic segment plays an important role in positioning the emission profile. The red-shifted emission observed for naphthyl and phenanthrenyl complexes may be associated with the comparatively weaker ligand field strength of the aryl units. It is interesting to note here that thienyl and benzothiophenyl complexes displayed batho-

(30) (a) Wang, Y.; Herron, N.; Grushin, V. V.; LeCloux, D.; Petrov, V. *Appl. Phys. Lett.* **2001**, *79*, 449. (b) Garces, F. O.; King, K. A.; Watts, R. J. *Inorg. Chem.* **1998**, *27*, 3464.

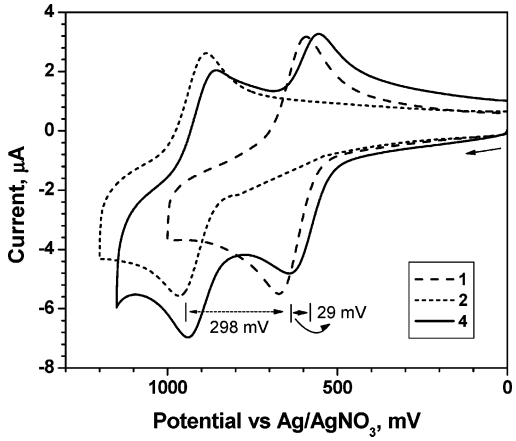

Figure 6. Cyclic voltammograms of complexes $Ir(BuL)_2(acac)$ (**1**), $Ir(CF_3L)_2(acac)$ (**2**), and $Ir(NPh_2L)_2(acac)$ (**4**) recorded in dichloromethane. Scan rate: 100 mV/s.

chromic shifts in the emissions when compared to the corresponding phenyl analogues.[31] Moderate to high quantum efficiencies were observed for the complexes. Normally orthometalated iridium complexes are known to have the highest triplet quantum yields due to several factors:[7] (a) Iridium normally undergoes large d-orbital splitting compared to other metals in the series. (b) The strong ligand field strength of the aromatic anion ligand increases the energy between the t_{2g} and e_g orbitals, leading to an enhanced gap between the e_g and LUMO of the ligand. (c) Close-lying $\pi-\pi^*$ and MLCT states together with the heavy atom effect enhance the spin−orbit coupling. Moderate quantum efficiencies realized for our complexes is noteworthy and may be ascribed to the combination of one more factors enumerated above. Comparatively low phosphorescence yield observed for dimethylamino-substituted complex **3** may be attributed to the intramolecular electron-transfer quenching of the excited state by dimethylamino units. This speculation is reasonable as this complex possesses two oxidation couples with lowest oxidation potentials in the series (Table 3). Considering low quantum efficiency for the NMe_2-substituted complex **3**, it is expected to display smaller excited-state lifetime. Contrary to this belief, we observed a long lifetime for this complex in this series. This may be ascribed to the predominant ^{3}IL ($\pi \rightarrow \pi^*$ (NMe_2L^-) character of the excited state, although the mixing of MLCT cannot be excluded.[32]

Electrochemical Studies. All the complexes exhibit a one-electron reversible oxidation couple at relatively low positive potentials (Table 3). None of the ligands display oxidation waves in this potential region (see Figure S2 in the Supporting Information). Thus, we attribute this low positive oxidation potential to the Ir centered oxidation. Additional reversible oxidation couple is also noticed in the complexes

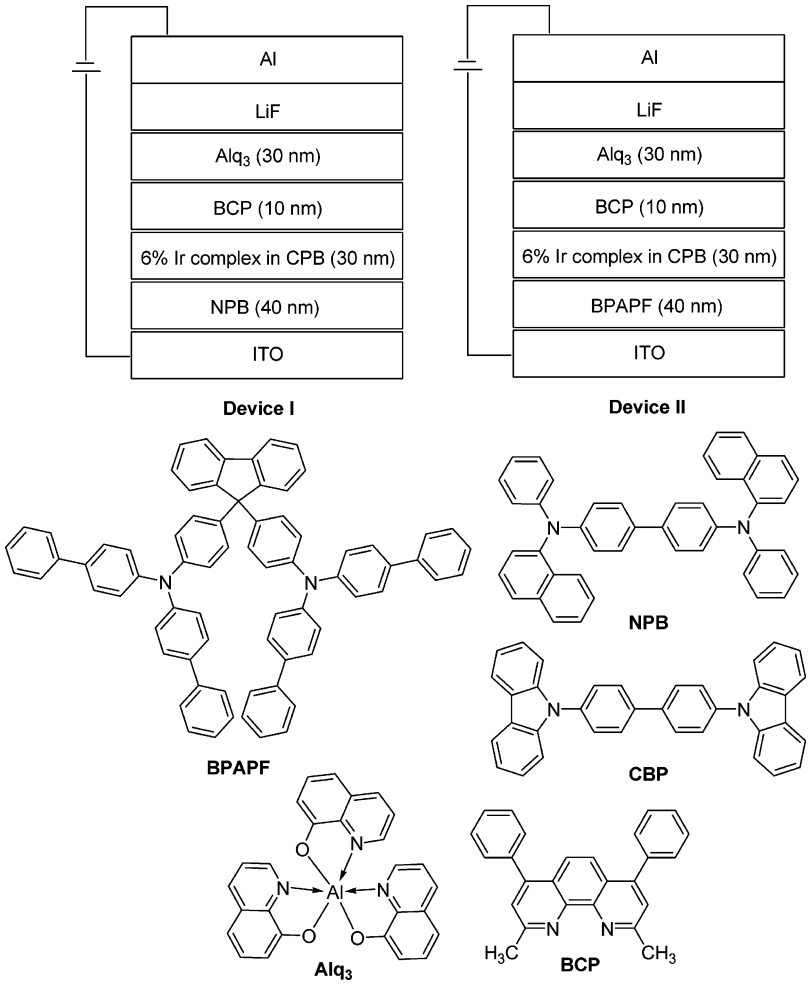

Figure 7. Device configurations and structure of the materials.

3 and **4**, which originates from the amine unit. The corresponding ligands NMe_2L and NPh_2L also displayed oxidation waves at 0.45 V (irreversible) and 0.53 V (reversible, $\Delta E_p = 76$ mV), respectively. Changes in the electron-donating and electron-withdrawing nature of the ligands may result in the variation in the electronic properties at the metal center, which in turn will be manifested on the redox propensity of the complexes.[7,19] It is interesting to compare the complexes **1**−**4** that contain *tert*-butyl, CF_3, and amino functionality, respectively, in the phenyl ring. The electron-withdrawing CF_3 group significantly shifts the Ir couple positively ($\Delta E_{1/2} = 298$ mV) in complex **2**, while a negative shift ($\Delta E_{1/2} = 138$ and 29 mV for **3** and **4**) for the electron-donating amino substituents is seen in **3** and **4** when compared to **1** (Figure 6). The larger positive shift for the CF_3-substituted ligand-containing complex **2** arises from the diminished electron density on Ir center due to the electron-withdrawing effect of CF_3. Observed oxidation potentials suggest that the phenanthrenyl unit is more electron-rich when compared to the *tert*-butyl- and diphenylamino-substituted phenyl ligands (compare complex **6** vs **1** and **4**). In complexes **1**−**6**, no reversible reduction waves due to the ligands were observed in dichloromethane. However, significant reduction currents above −1.8 V are visible in the cyclic voltammogram, which were not analyzed in detail.

Light-Emitting Diodes. The complexes described here possess red-shifted emission and moderate to good triplet quantum efficiencies. In view of the recent surge in the search of suitable triplet dopants for the fabrication of light-emitting diodes, we have also examined the possibility of using these complexes as emitting guests in LED devices. Two types of electroluminescent devices of the configurations ITO/NPB (40 nm)/6% **1**−**6** in CBP (30 nm)/BCP (10 nm)/Alq_3 (30 nm)/LiF/Al (device I) and ITO/BPAPF (40 nm)/6% **1**−**6** in CBP (30 nm)/BCP (10 nm)/Alq_3 (30 nm)/LiF/Al (device II) were fabricated (Figure 7). We have used CBP as the host for the iridium complexes because of its proven earlier performance as host for iridium complexes and theoretical confirmation of favorable triplet energy.[33] It is necessary to introduce a hole-blocking layer (HBL), BCP, into our device composition to confine the recombination zone inside the doped CBP layer; without the HBL the recombination takes place inside the Alq_3 layer (emission maximum at 530 nm wavelength). This indicates that with HBL the emission takes place in CBP just near the CBP/BCP interface as the electron are entering CBP. We have also examined the influence of the hole-transporting layer by replacing NPB with a fluorene derivative, BPAPF, which possesses excellent thermal properties and hole injection capabilities. Because of these meticulous designs, all the devices led to intense orange or red emission originating from the iridium complexes. The device characteristics are listed in Table 4, and the $I-V-L$ trends are displayed in Figures 8−10. The close resemblance between the PL and EL spectra indicates the absence of aggregation or π-stacking up to 6% doping level.

Table 4. Electroluminescence Data for the Devices[a]

complex	λ_{EL}/nm (fwhm)	CIE x, y	V_{ON}/ V	L_{max}/ cd m^{-2}	L_{100}[b]/ cd m^{-2}	V_{100}[b]/ V	η[b]/ %	η_c[b]/ cd A^{-1}	η_p[b]/ lmW^{-1}
1	598 (60)	0.59, 0.39	3.5	61 750	19 500	11.86	8.84	19.61	5.20
	598 (62)	0.60, 0.39	4.0	72 130	26 260	12.36	12.11	26.37	6.71
2	586 (68)	0.56, 0.43	5.0	38 200	11 800	11.70	4.73	11.92	3.21
	586 (70)	0.57, 0.43	4.5	38 560	12 250	10.72	5.02	12.32	3.61
3	600 (66)	0.61, 0.39	4.5	19 050	13 150	13.87	6.85	13.22	3.00
	602 (66)	0.61, 0.39	5.0	14 380	5 080[c]	12.98[c]	13.15[c]	25.00[c]	6.02[c]
4	596 (62)	0.59, 0.40	4.5	19 150	13 000	13.91	6.05	13.05	2.95
	594 (62)	0.60, 0.40	4.5	16 850	16 060	14.87	7.63	16.16	3.42
5	638 (50)	0.69, 0.30	4.0	13 000	5 200	12.31	7.92	5.22	1.33
	638 (52)	0.69, 0.30	4.0	7 350	6 000	14.53	9.06	6.00	1.30
6	664 (52)	0.68, 0.29	4.5	2 900	2 300	14.37	9.32	2.31	0.50
	664 (52)	0.71, 0.29	4.5	2 330	2 320	14.98	9.78	2.32	0.49

[a] For each compound the first column gives the data for device I and the second column is for device II. [b] At current density 100 mA/cm^2. [c] At current density 20 mA/cm^2.

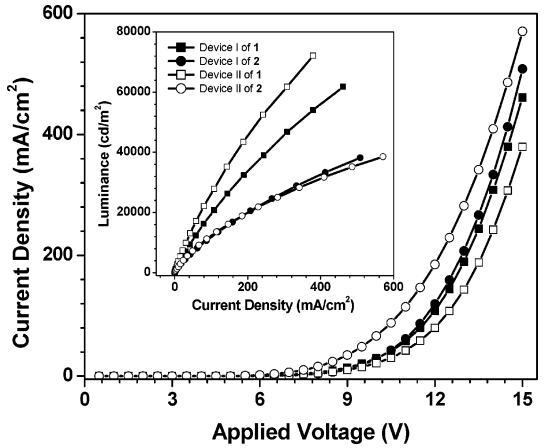

Figure 8. $I-V-L$ characteristics of the devices fabricated using $Ir(BuL)_2(acac)$ (**1**) and $Ir(CF_3L)_2(acac)$ (**2**).

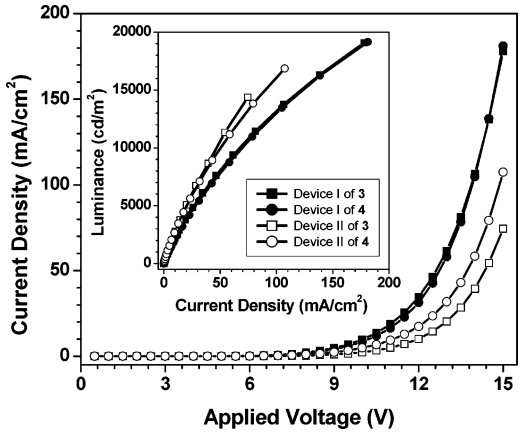

Figure 9. $I-V-L$ characteristics of the devices fabricated using $Ir(NMe_2L)_2(acac)$ (**3**) and $Ir(NPh_2L)_2(acac)$ (**4**).

In general device I of the complexes displays higher current densities than that of device II with the exception of the compound **2**. On the contrary, device II appears to have

(31) Adachi, C.; Baldo, M. A.; Forrest, S. R.; Lamansky, S.; Thompson M. E.; Kwong, R. C. *Appl. Phys. Lett*. **2001**, *78*, 1622.

(32) (a) Yersin, H. *Top. Curr. Chem*. **2004**, *241*, 1. (b) Lo, K. K.-W.; Chan, J. S.-W.; Chung, C.-K.; Tsang, V. W.-H.; Zhu, N. *Inorg. Chim. Acta* **2004**, *357*, 3109. (c) Hay, P. J. *J Phys. Chem. A* **2002**, *106*, 1634.

(33) (a) D'Andrade, B. W.; Baldo, M. A.; Adachi, C.; Brooks, J.; Thompson, M. E.; Forrest, S. R. *Appl. Phys. Lett*. **2001**, *79*, 1045. (b) Adachi, C.; Kwong, R. C.; Djurovich, P.; Adamovich, V.; Baldo, M. A.; Thompson, M. E.; Forrest, S. R. *Appl. Phys. Lett*. **2001**, *79*, 2082. (c) Baldo, M. A.; Thompson, M. E.; Forrest, S. R. *Nature* **2000**, *403*, 750.

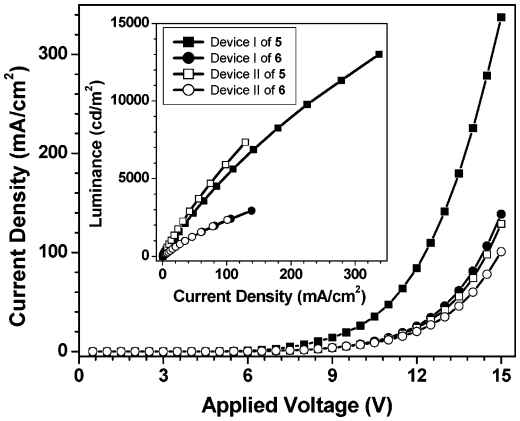

Figure 10. *I*−*V*−*L* characteristics of the devices fabricated using Ir(NapL)$_2$(acac) (**5**) and Ir(PhenL)$_2$(acac) (**6**).

better performance than device I. It is pointed out by Thompson et al. that the iridium complexes also contribute to the transport of charges. Therefore, there is better balance of electron and hole transport rates inside the emitting layer of device II. The CIE coordinates observed for the devices I are plotted in Figure 11. Devices II also display identical CIE patterns. Most of the devices appear in the red region, while the diodes derived from **1**, **3**, and **4** are close to the NTSC standards. The performance of the saturated red-emitting devices derived from the complexes **3** and **5** are promising. Another characteristic of phosphorescent dye doped OLEDs described here is that the maximum of the external quantum efficiency (QE) is located at low voltages (9−10 V) and that for higher voltages a strong decrease in the QE is seen. This kind of decrease is discussed as arising from a triplet−triplet annihilation effect.[34]

Summary

In summary, we have synthesized and characterized a new series of lepidine-based iridium(III) complexes that are bright red emitters and suitable for red electroluminescent devices. Crystal structures of the three complexes were performed by single-crystal X-ray diffraction, and the structural parameters were compared with the related cyclometalated iridium(III) acetylacetonate complexes. The optical properties of the complexes were critically analyzed and related to the ligand field strength of the aryl anion ligands involved. The redox propensity of the iridium complexes were influenced by the electron-donating substituents present on the cyclometalating aryl unit. Bright red-emitting electroluminescent devices were constructed using the iridium(III) complexes as doped emitters. Variation of the dopant concentration to achieve optimized and stabilized electroluminescent properties in devices for this class of complexes will be studied in the future.

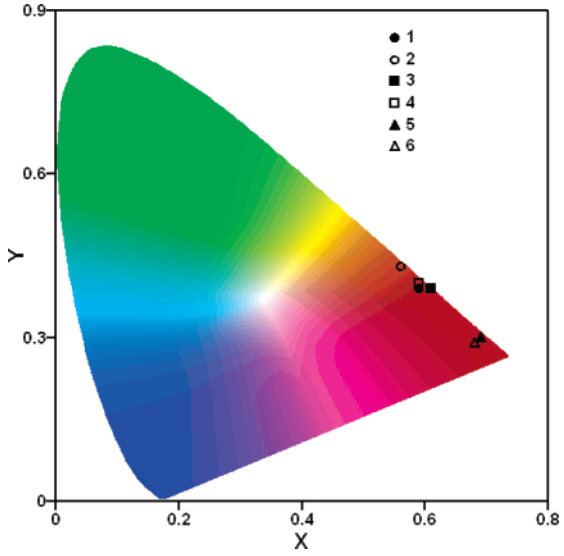

Figure 11. CIE 1931 coordinates plot for device I.

Acknowledgment. We thank the Academia Sinica and National Science Council for financial support.

Supporting Information Available: Crystallographic information files for complexes **2**, **3**, and **5**, absorption spectra of the ligands, and CV traces of the ligands. This material is available free of charge via the Internet at http://pubs.acs.org.

IC050385S

(34) Baldo, M. A.; Adachi, C.; Forrest, S. R. *Phys. Rev. B* **2000**, *62*, 10967.